Resonance Raman Studies on Protocatechuate 3,4-Dioxygenase–Inhibitor Complexes†

Lawrence Que, Jr.,* and Robert M. Epstein

ABSTRACT: Resonance Raman spectra of a number of protocatechuate 3,4-dioxygenase–inhibitor complexes were studied by use of the available lines of an argon and a krypton laser. Three types of inhibitors were investigated—hydroxybenzoates, dicarboxylates, and 4-nitrocatechol. The hydroxybenzoate study shows that the hydroxy group in 3-hydroxybenzoate does not coordinate to the active site iron, in agreement with earlier suggestions, and confirms the coordination of the hydroxy group in the isomeric 4-hydroxybenzoate. The dicarboxylate study demonstrates that both glutarate and terephthalate perturb the active-site environment, shifting the charge-transfer interaction to lower energy. The pH dependence of terephthalate binding as well as the spectral similarities of the dicarboxylate complexes to the ESO_2 intermediate provides further evidence for the suggestion that this intermediate is a tightly bound enzyme–product complex. The 4-nitrocatechol study indicates that, unlike the substrate catechols, 4-nitrocatechol does not bind to the iron; a binding configuration wherein the acidic phenolate group interacts with the carboxylate binding site has been suggested by others. Finally the spectra of the 4-hydroxybenzoate and terephthalate complexes demonstrate the presence of two tyrosines coordinated to the active-site iron as suggested by others; these tyrosines have different ν_{CO}'s and excitation profiles.

Protocatechuate 3,4-dioxygenase [PCD; 3,4-dihydroxybenzoate:oxygen oxidoreductase (decyclizing), EC 1.3.11.3] belongs to a class of non-heme iron enzymes which catalyze the cleavage of catechols to *cis,cis*-muconic acids (Nozaki, 1974; Que, 1980). Resonance Raman studies on these enzymes have demonstrated tyrosinate coordination to the iron, giving rise to a charge-transfer band in the visible region with an absorbance maximum near 460 nm (Tatsuno et al., 1978; Keyes et al., 1978; Felton et al., 1978; Bull et al., 1979; Que & Heistand, 1979). The spectra are characterized by four marker bands at ca. 1175, 1270, 1505, and 1605 cm^{-1}; these have been assigned to a bending mode, the C–O stretch, and two ring breathing modes involving mainly C–C stretches, respectively. Similar spectroscopic properties have been found for various transferrins (Gaber et al., 1974, 1979; Tomimatsu et al., 1976; Ainscough et al., 1980); these properties appear to be characteristic of a new class of iron proteins with tyrosinate coordination (Keyes et al., 1978). We have investigated the resonance Raman spectra of several inhibitor complexes of protocatechuate 3,4-dioxygenase; these spectra provide more insight into the enzyme active site and its interaction with ligands.

Materials and Methods

All chemicals were obtained commercially and used without further purification. Deuteration of the positions ortho and para to the hydroxyl group in 3HB and 4HB was effected by base-catalyzed exchange in D_2O under N_2 in a sealed NMR tube heated at 140 °C for 10 h. The NMR spectra of the resulting solutions showed >95% deuteration.

PCD was prepared from *Pseudomonas aeruginosa* (ATCC 23975) according to published procedures (Fujisawa et al., 1972a; May et al., 1978). The crystalline enzyme had a specific activity of 65 or better. Steady-state inhibition kinetic experiments were performed on a Gilson K-1C oxygraph at 25 °C.

Visible spectra were obtained on a Cary 219 spectrophotometer. Resonance Raman spectra were obtained using a Coherent Radiation Model CR-3 argon ion laser and Model 500K krypton ion laser. The spectra were recorded on a SPEX 1401 spectrometer interfaced with a microprocessor for data handling. Spectra were obtained on 40–50 mg/mL protein samples at 4 °C and sulfate was used as an internal standard. Excitation profile intensities were obtained by comparisons of band peak heights with that of the sulfate standard. The Raman data are given in Table I together with relevant information from previous studies.

Results

Hydroxybenzoates. Hydroxybenzoates are competitive inhibitors of protocatechuate 3,4-dioxygenase; steady-state kinetic studies of these inhibitor complexes indicate that the *p*-hydroxybenzoates are much better inhibitors than the corresponding *m*-hydroxybenzoates (Que et al., 1977; May et al., 1978). These observations have led to suggestions that this difference in binding affinities arises from the binding of the *p*-hydroxy group to the iron and the absence of such an interaction for the *m*-hydroxy group. We have thus compared the resonance Raman spectra (Figure 1) of PCD complexes with 4-hydroxybenzoate (4HB)[1] and 3-hydroxybenzoate (3HB). The spectrum of the PCD–3HB complex closely resembles that of the native enzyme; in addition, nonresonance modes of the inhibitor are observed at 1004 and 1396 cm^{-1} due to the high concentrations of inhibitor required to saturate the active site. Deuteration of the C-2, C-4, and C-6 protons of the inhibitor does not alter the observed spectrum. In contrast, the PCD–4HB complex exhibits a spectrum with two additional features in the ν_{CO} region and a shoulder at 1597 cm^{-1}. Deuteration of the C-3 and C-5 protons of 4HB results in the shift of the peaks at 1276 and 1597 cm^{-1} to 1267 and 1586 cm^{-1}, thus identifying these features as arising from the inhibitor.

The spectrum of the PCD–4HB complex is also in striking contrast to previously reported spectra of PCD complexed with 3-fluoro-4-hydroxybenzoate (3FHB) and 3-chloro-4-

† From the Department of Chemistry, Baker Laboratory, Cornell University, Ithaca, New York 14853. *Received June 17, 1980.* This work was supported by the National Institutes of Health Grant GM25422.

[1] Abbreviations used: PCD, protocatechuate 3,4-dioxygenase; 3HB, 3-hydroxybenzoate; 4HB, 4-hydroxybenzoate; 3FHB, 3-fluoro-4-hydroxybenzoate; 3ClHB, 3-chloro-4-hydroxybenzoate; CD, circular dichroism; 4NC, 4-nitrocatechol.

0006-2960/81/0420-2545$01.25/0

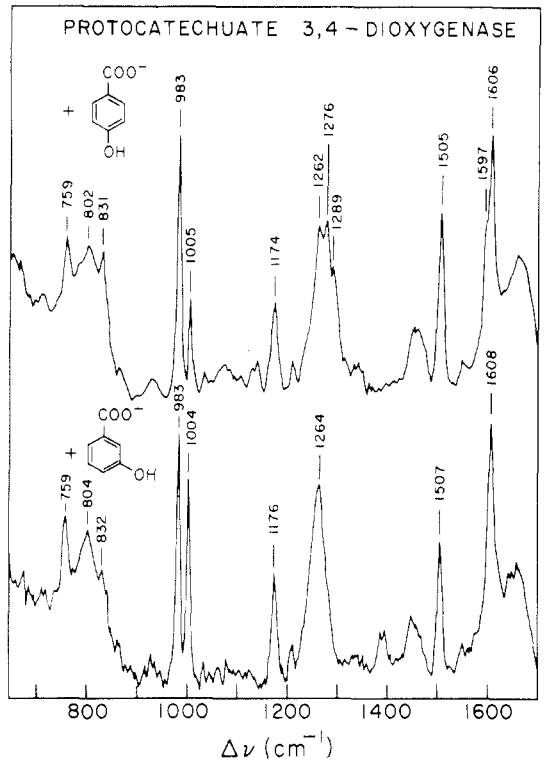

FIGURE 1: Resonance Raman spectra of the PCD–4HB complex (top) and the PCD–3HB complex (bottom). Conditions: 488.0-nm excitation, 100–150-mW power, 4-cm^{-1} slit width. 4HB concentration, 2 mM; 3 HB concentration, 50 mM; 50 mM Tris-Cl buffer, pH 8.5.

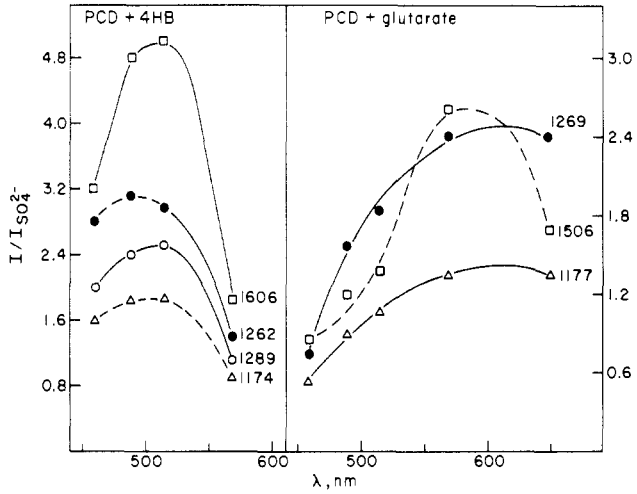

FIGURE 2: Excitation profiles of the PCD–4HB complex (left) and the PCD–glutarate complex (right). Data points are band peak heights normalized to the 983-cm^{-1} band of SO_4^{2-} (0.1 M).

hydroxybenzoate (3ClHB). Whereas the 3FHB and 3ClHB spectra exhibit a ν_{CO} region with two peaks, one twice as intense as the other, the 4HB spectrum has a ν_{CO} region consisting of three peaks of nearly equal intensity. Since the 1276-cm^{-1} feature has been assigned to the inhibitor, the remaining two must arise from the enzyme. We have also obtained the excitation profile of the PCD–4HB complex (Figure 2), which shows maximum enhancement for all peaks near 500 nm, coincident with the weak positive band in its CD spectrum (Zaborsky et al., 1975).

Dicarboxylates. We have also investigated the spectral properties of the glutarate and the terephthalate (*p*-benzenedicarboxylate) complexes of PCD. Both are competitive inhibitors of the enzyme, with K_i's of 15 and 6 mM, respectively, at pH 7.5. The visible spectra of the complexes

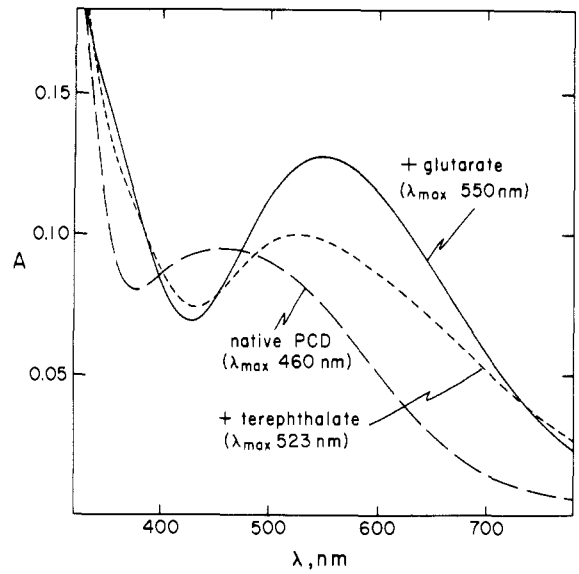

FIGURE 3: Visible absorption spectra of native PCD, the PCD–terephthalate complex, and the PCD–glutarate complex. Spectra were obtained on 2.4 mg/mL enzyme in 50 mM potassium phosphate buffer, pH 7.5, 25 °C. Terephthalate concentration, 0.1 M; glutarate concentration, 0.2 M.

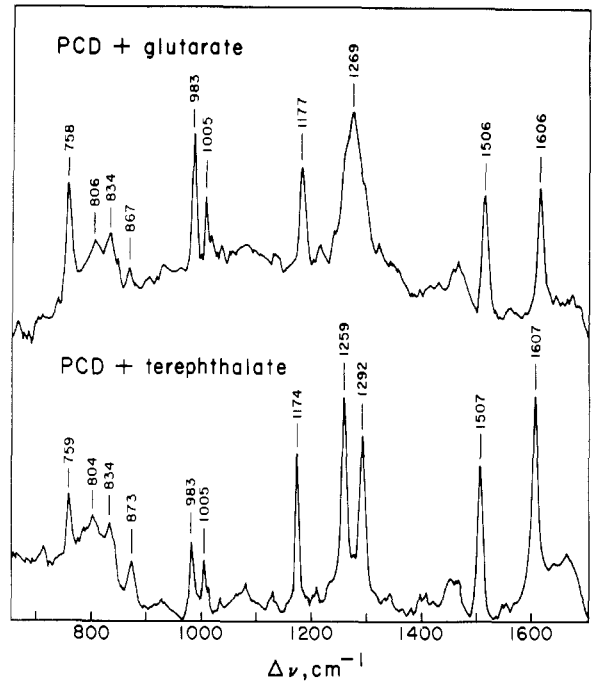

FIGURE 4: Resonance Raman spectra of the PCD–glutarate complex (top) and the PCD–terephthalate complex (bottom). Conditions: 514.5-nm excitation, 100–150-mW power, 4-cm^{-1} slit width. Glutarate concentration, 100 mM in 50 mM Tris-Cl buffer, pH 8.5; terephthalate concentration, 20 mM in 50 mM potassium phosphate buffer, pH 7.

(Figure 3) show large red shifts in the absorbance maxima, similar to that observed for the benzoate complex of catechol 1,2-dioxygenase (Que et al., 1980). Presumably for the PCD complexes, one carboxylate binds at the carboxylate binding site (an arginine residue; Carlson et al., 1980) and the other coordinates to the iron, inducing the red shift.

The resonance Raman spectrum of the glutarate complex (Figure 4, top) exhibits the familiar tyrosine vibrational modes of the native enzyme; the 1269-cm^{-1} band, which is assigned to the ν_{C-O}, is particularly broad and somewhat asymmetric. No resonance-enhanced inhibitor modes are observed since carboxylate-to-iron charge transfer interactions would not be

Table I: Resonance Raman Data for Dioxygenase Complexes (700–1700 cm^{-1})

enzyme complex	excitation wavelength (nm)	observed modes (cm^{-1})												ref
protocatechuate 3,4-dioxygenase														
native	488.0, 514.5	1605		1505				1265	1176		863	834	756	*a–d*
+DHPP	514.5	1604		1502	1471	1318		1265	1174				760	*c*
+catechol	647.1				1470	1323		1255						*e*
+DHPP + O_2	530.9							1252	1165		864	833		*f*
+4HB	514.5	1606	1597	1505		1277	1289	1262	1174		831	802	759	*g*
+4HB-*3,5-d*$_2$	514.5	1607	1586	1506			1292	1267	1174					*g*
+3HB	488.0	1608		1508				1264	1176		832	804	759	*g*
+3ClHB	514.5	1606	1592	1505	1487	1299		1260	1171				759	*c, g*
+3FHB	514.5	1606		1505		1303		1263	1173				760	*c*
+glutarate	514.5	1606		1506				1269	1177	867	834	806	758	*g*
+terephthalate	514.5	1609		1507			1293	1259	1175	873	834	804	759	*g*
+4NC	488.0	1607	1564		1457	1344	1267	1207	1192	1083	953	787	757	
catechol 1,2-dioxygenase														
native	647.1	1604		1506			1289		1175				757	*h*
+catechol	647.1				1481	1321		1263						*e*
+4NC	647.1				1494	1331	1322	1288	1255		829	806		*e*
+*o*-chlorophenol	514.5	1605	1586	1505	1475	1300		1260	1175		874	802	762	*h*
	647.1	1605		1507		1301	1289	1260	1175		875		761	*h*
+benzoate	514.5	1604		1506			1297	1258	1175		876		762	*h*

[a] Tatsuno et al. (1978). [b] Keyes et al. (1978). [c] Felton et al. (1978). [d] Bull et al. (1979). [e] Que & Heistand (1979). [f] Keyes et al. (1979). [g] This work. [h] Que et al. (1980).

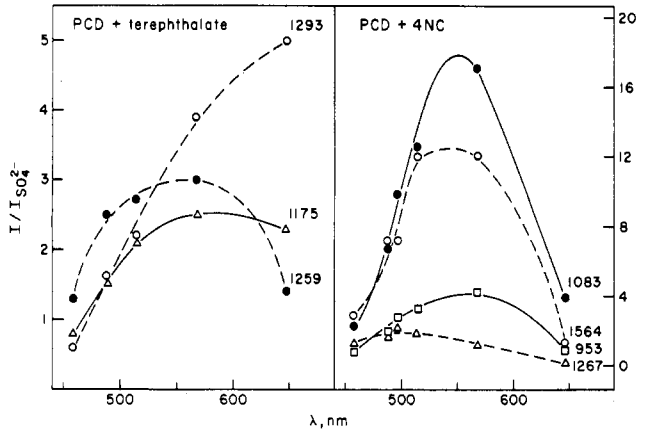

FIGURE 5: Excitation profiles of the PCD–terephthalate complex (left) and the PCD–4NC complex (right). Data points are band peak heights normalized to the 983-cm^{-1} band of SO_4^{2-} (0.1 M).

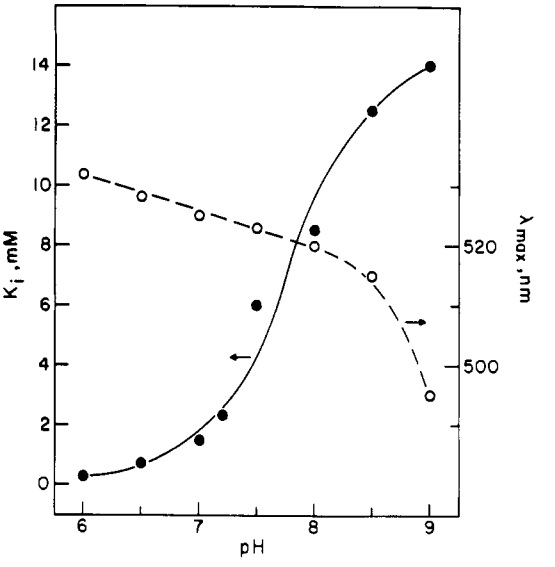

FIGURE 6: pH dependence of the K_i's and the λ_{max}'s of the PCD–terephthalate complex in 50 mM Tris–phosphate buffer. Terephthalate concentration, 100 mM, for the visible spectra.

expected to occur in the visible region. The excitation profile of this complex (Figure 2) shows maximum enhancement of all features near 600 nm.

The terephthalate complex has been investigated in greater detail. Its resonance Raman spectrum (Figure 4, bottom) also exhibits only enzyme vibrational modes; the ν_{CO} region, interestingly, shows two symmetric peaks at 1259 and 1292 cm^{-1}. (Nonresonant terephthalate modes are observed at 1131, 1406, and 1611 cm^{-1} in concentrated terephthalate solutions, so neither peak is assignable to the inhibitor.) The excitation profile of the terephthalate complex is shown in Figure 5. The 1259-cm^{-1} band peaks near 560 nm and the 1293-cm^{-1} band peaks above 650 nm, while the remaining bands (represented by the 1175-cm^{-1} feature) maximize around 600 nm.

In the course of our investigation, we noticed that the visible spectrum of the terephthalate complex was pH dependent (Figure 6). The complex exhibits a λ_{max} at 532 nm at pH 6 and one at 495 nm at pH 9. Resonance Raman spectra obtained at pH 7 and 8.5 show no change in peak positions, though the excitation profile of the 1259-cm^{-1} peak exhibits a slight blue shift at the higher pH. The ionization of some residue in the active site thus appears to modulate the tyrosine-to-iron charge-transfer interaction. This pH dependence of the visible spectrum has also been observed for the glutarate complex but not for the *p*-hydroxybenzoate complex.

Because the shift in the absorbance maximum may reflect a change in binding affinity, we have also investigated the pH dependence of the kinetically determined K_i for terephthalate. This pH dependence has an apparent pK_a of 7.8 (Figure 6), which differs from the pH dependence of the absorbance maximum and suggests that the protonation of a different active-site residue facilitates inhibitor binding.

4-Nitrocatechol. 4-Nitrocatechol has been used as a colorimetric probe for the dioxygenases (Tyson, 1975). It is a good competitive inhibitor of PCD (K_i = 1 μM), and its complex with PCD exhibits a visible spectrum with peaks at 410 and 550 nm, remarkably similar to that of the dianion. The resonance Raman spectrum of the PCD–4NC complex is dominated by the 4NC chromophore, with features resembling those found in the dianion spectrum (Figure 7). In addition, features arising from the enzyme can be observed at 1264 and 1607 cm^{-1}. The excitation profiles for selected

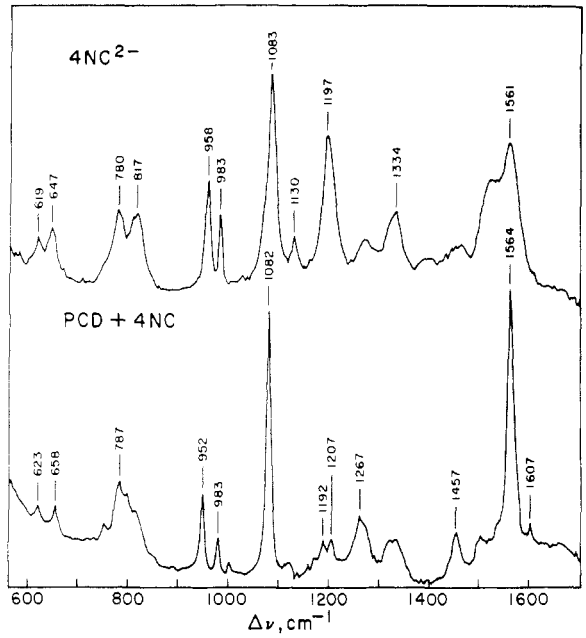

FIGURE 7: Resonance Raman spectra of the 4NC dianion (top) and the PCD–4NC complex (bottom). Conditions: 488-nm excitation, 100-mW power, 4-cm^{-1} slit width. 4NC concentration for both samples, 0.5 mM.

peaks are shown in Figure 5. The 953- and 1083-cm^{-1} features maximize near the absorbance maximum while the 1564-cm^{-1} band peaks at slightly lower wavelength. These features arise from the 4NC chromophore; the corresponding peaks in the 4NC dianion spectrum exhibit analogous excitation profiles. The 1267-cm^{-1} band, on the other hand, maximizes near 500 nm. This band is most likely a composite of features from both enzyme and 4NC, but its excitation profile suggests that the band is dominated by the enzyme chromophore. The excitation maximum should have been closer to 550 nm if the 4NC chromophore were the major component. The profile of the 1607-cm^{-1} (not shown) peak which is unequivocally assigned to the enzyme also exhibits a maximum near 500 nm.

Discussion

Protocatechuate 3,4-dioxygenase interacts with a variety of substrate and product analogues, giving rise to interesting spectral changes. Using resonance Raman spectroscopy, we have studied the complexes of PCD with hydroxybenzoates, dicarboxylates, and 4-nitrocatechol and obtained insights into the iron coordination of the enzyme.

The resonance Raman spectra of PCD and many of its complexes are characterized by four marker bands, which have been assigned to tyrosinate vibrations. In the spectra of the 4HB and the terephthalate complexes, we have observed the emergence of a new feature near 1290 cm^{-1}. The excitation profile of this feature in the terephthalate complex is distinct from the profiles of the other peaks, suggesting that it arises from a different electronic transition.

There are two possible assignments for the 1290-cm^{-1} peak—an imidazole breathing mode and a tyrosine ν_{CO}. Imidazole is readily eliminated because imidazole modes are normally observed near 1260 cm^{-1}. Furthermore, experiments in D_2O (Felton et al., 1978) have failed to show detectable shifts in the observed spectra; a 13-cm^{-1} shift is expected when the N-1 proton of imidazole is deuterated (Salama & Spiro, 1978).

The ~1290-cm^{-1} peak is thus assigned to the ν_{CO} of a tyrosine, meaning that there are two tyrosines coordinated to the active-site iron exhibiting different ν_{CO}'s. That the other tyrosinate modes are not likewise duplicated is not surprising because the ν_{CO} feature has been found to be quite variable from protein to protein with the other three marker bands remaining relatively constant (Gaber et al., 1979). Similar conclusions have been made for the tyrosine coordination in catechol 1,2-dioxygenase (Que et al., 1980). In contrast to the observations on catechol 1,2-dioxygenase, only the 4HB and terephthalate complexes of PCD exhibit this differentiation of the two tyrosines; all other PCD complexes studied so far show only one ν_{CO} feature. It appears that this differentiation results from the binding of a para-substituted benzoate with no meta substitution. Why this should be so is not presently understood.

The two-tyrosine postulate for the active-site coordination in PCD is not unique to this work. Felton et al. (1978) previously suggested this possibility on the basis of intensity comparisons in their study of the halohydroxybenzoate complexes. Indeed, a comparison of their spectra for the 3FHB and 3ClHB complexes with our data on the 4HB complex reveals a rather consistent picture. In the halohydroxybenzoate complexes, the two tyrosines exhibit the same ν_{CO}, giving rise to a peak with approximately twice the intensity of the ν_{CO} from the bound inhibitor. In the 4HB complex, the tyrosines have somehow become differentiated, and three ν_{CO}'s of nearly equal intensity are observed.

The possibility that the two features in the ν_{CO} region may originate from the same tyrosine has also been considered. This, however, was thought unlikely on the basis of the excitation profiles of the dicarboxylate complexes. In the glutarate complex where only one ν_{CO} is observed, all features show excitation maxima near 600 nm. In the terephthalate complex, the two ν_{CO}'s peak near 560 and 650 nm, respectively, indicating the presence of two electronic transitions. The other marker bands maximize near 600 nm, consistent with these features being composites of the two tyrosines.

Our studies with inhibitors have also provided some insights into how these species interact with the active site. Our hydroxybenzoate study provides the definitive proof for earlier suggestions that the hydroxy group in 4HB binds to the iron while that in 3HB does not. This conclusion stems from the observation of resonance-enhanced modes assignable to 4HB in the PCD–4HB complex and the absence of similar features in the 3HB complex. Whether this conclusion can be extended to the substrate interaction remains an open question since the spectra of enzyme–substrate complexes resemble those of synthetic complexes with chelated catecholates (Felton et al., 1978; Que & Heistand, 1979). We are continuing this investigation.

The binding of dicarboxylates to PCD induces red shifts in the visible spectra of these complexes. These spectra resemble that reported for the oxygenated intermediate (Fujisawa et al., 1972b) which exhibits a maximum near 520 nm. Furthermore, the pH dependence for the binding of terephthalate exhibits a pK_a similar to those for the k_{cat} of protocatechuate and the decomposition of the ESO_2 intermediate formed with DHPP (May & Phillips, 1979). Nakata et al. (1978) have suggested that the purple ESO_2 intermediate may be a tightly bound enzyme–product complex. The pH dependence of terephthalate binding is consistent with this suggestion, i.e., tighter binding at low pH leading to slower product release. Though we earlier suggested the formulation of the ESO_2 intermediate as an iron–peroxide complex (Que et al., 1977), the accumulated evidence (Nakata et al., 1978; Keyes et al., 1979; Ballou & Bull, 1979) appears to favor a structure closer to the enzyme–product complex.

Finally, the spectral similarities of the PCD–4NC complex to the 4NC dianion indicate that both 4NC protons dissociate upon binding. This is consistent with our studies on the enzyme–substrate complexes, where the catecholates bind as dianions (Que & Heistand, 1979). Furthermore, the red shift in the absorbance maximum reflects a change in environment, probably to a more hydrophobic one. Indeed, a DMF solution of the dianion exhibits a visible spectrum with a peak at 554 nm.

The striking aspect of the resonance Raman spectrum of the PCD–4NC complex is the absence of features typical of catecholate binding to the iron. Such an interaction is characterized by Raman peaks at ca. 1260, 1320, and 1480 cm^{-1}, with the 1480-cm^{-1} band most prominent. These bands have been observed in the enzyme–substrate complexes of PCD and catechol 1,2-dioxygenase as well as synthetic iron complexes (Felton et al., 1978; Salama et al., 1978; Que & Heistand, 1979). Similar features are also found in the spectrum of the catechol 1,2-dioxygenase complex with 4NC. The absence of such features, the 1480-cm^{-1} peak in particular, in the spectrum of the PCD–4NC complex indicates that 4NC does not bind to the active-site iron like other catechols do. An alternative is a "backward" binding configuration such that the acidic phenolate oxygen interacts with the carboxylate binding site, proposed by May et al. (1978). This possibility is intriguing, but it suggests that the sole requirement for strong binding is the inhibitor's capability of interacting with the arginine residue. Thus, various benzoates would be expected to be as good inhibitors, which they are not. Other factors must be involved in the 4NC binding. We have determined that both hydroxy groups are required for this strong affinity since *m*- and *p*-nitrophenol are much poorer inhibitors of PCD (M. J. Eisenberg, and L. Que, Jr., unpublished observations). But the picture is still incomplete, and we are continuing this investigation.

In conclusion, resonance Raman spectroscopy has been an excellent tool for probing active-site interactions in the catechol dioxygenases. Details of these interactions provide a better understanding of the enzyme structure and function.

Acknowledgments

We thank Professor H. A. Scheraga for the use of the Raman spectrometer and M. J. Eisenberg for experimental assistance.

References

Ainscough, E. W., Brodie, A. M., Plowman, J. E., Bloor, S. J., Loehr, J. S., & Loehr, T. M. (1980) *Biochemistry 19*, 4072–4079.

Ballou, D., & Bull, C. (1979) in *Biochemical and Clinical Aspects of Oxygen* (Caughey, W., Ed.) pp 573–587, Academic Press, New York.

Bull, C., Ballou, D. P., & Salmeen, I. (1979) *Biochem. Biophys. Res. Commun. 87*, 836–841.

Carlson, R. E., Wood, J. M., & Howard, J. B. (1980) *Fed. Proc., Fed. Am. Soc. Exp. Biol. 39*, 2090.

Felton, R. H., Cheung, L. D., Phillips, R. S., & May, S. W. (1978) *Biochem. Biophys. Res. Commun. 85*, 844–850.

Fujisawa, H., Uyeda, M., Kojima, G., Nozaki, M., & Hayaishi, O. (1972a) *J. Biol. Chem. 247*, 4414–4421.

Fujisawa, H., Hiromi, K., Uyeda, M., Okuno, S., Nozaki, M., & Hayaishi, O. (1972b) *J. Biol. Chem. 247*, 4422–4428.

Gaber, B. P., Miskowski, V., & Spiro, T. G. (1974) *J. Am. Chem. Soc. 96*, 6868–6873.

Gaber, B. P., Sheridan, J. P., Bazer, F. W., & Roberts, R. M. (1979) *J. Biol. Chem. 254*, 8340–8342.

Keyes, W. E., Loehr, T. M., & Taylor, M. L. (1978) *Biochem. Biophys. Res. Commun. 83*, 941–945.

Keyes, W. E., Loehr, T. M., Taylor, M. L., & Loehr, J. S. (1979) *Biochem. Biophys. Res. Commun. 89*, 420–427.

May, S. W., & Phillips, R. S. (1979) *Biochemistry 18*, 5933–5939.

May, S. W., Phillips, R. S., & Oldham, C. D. (1978) *Biochemistry 17*, 1853–1860.

Nakata, H., Yamauchi, T., & Fujisawa, H. (1978) *Biochim. Biophys. Acta 527*, 171–181.

Nozaki, M. (1974) in *Molecular Mechanisms of Oxygen Activation* (Hayaishi, O., Ed.) pp 135–167, Academic Press, New York.

Que, L., Jr. (1980) *Struct. Bonding (Berlin) 40*, 39–72.

Que, L., Jr., & Heistand, R. H., II (1979) *J. Am. Chem. Soc. 101*, 2219–2221.

Que, L., Jr., Lipscomb, J. D., Munck, E., & Wood, J. M. (1977) *Biochim. Biophys. Acta 485*, 60–74.

Que, L., Jr., Heistand, R. H., II, Mayer, R., & Roe, A. L. (1980) *Biochemistry 19*, 2588–2593.

Salama, S., & Spiro, T. G. (1978) *J. Am. Chem. Soc. 100*, 1105–1111.

Salama, S., Stong, J. D., Neilands, J. B., & Spiro, T. G. (1978) *Biochemistry 17*, 3781–3785.

Tatsuno, Y., Saeki, Y., Iwaki, M., Yagi, T., Nozaki, M., Kitagawa, T., & Otsuka, S. (1978) *J. Am. Chem. Soc. 100*, 4614–4615.

Tomimatsu, Y., Kint, S., & Scherer, J. R. (1976) *Biochemistry 15*, 4918–4924.

Tyson, C. A. (1975) *J. Biol. Chem. 250*, 1765–1770.

Zaborsky, O. R., Hou, C. T., & Ogletree, J. (1975) *Biochim. Biophys. Acta 386*, 18–25.